BBA - Biomembranes 1860 (2018) 526–533

Contents lists available at ScienceDirect

BBA - Biomembranes

journal homepage: www.elsevier.com/locate/bbamem

Altered lipid properties of the stratum corneum in Canine Atopic Dermatitis

Suttiwee Chermprapai[a,b,c,*], Femke Broere[a,c], Gert Gooris[d], Yvette M. Schlotter[c], Victor P.M.G. Rutten[a,e], Joke A. Bouwstra[d]

[a] Department of Infectious Diseases and Immunology, Faculty of Veterinary Medicine, Utrecht University, Utrecht, The Netherlands
[b] Department of Companion Animals Clinical Sciences, Faculty of Veterinary Medicine, Kasetsart University, Bangkok, Thailand
[c] Department of Clinical Sciences of Companion Animals, Faculty of Veterinary Medicine, Utrecht University, Utrecht, The Netherlands
[d] Faculty of Science, Leiden Academic Centre for Drug Research, Cluster BioTherapeutics, Department of Drug Delivery Technology, The Netherlands
[e] Department of Veterinary Tropical Diseases, Faculty of Veterinary Science, University of Pretoria, Onderstepoort, South Africa

ARTICLE INFO

Keywords:
Stratum corneum
Lamellar organization
Lipid composition
Atopic dermatitis
Canine

ABSTRACT

Skin barrier disruption plays a role in the pathogenesis of atopic dermatitis (AD) in humans. However, little is known about skin barrier (dys-) function in Canine Atopic Dermatitis. The properties of lipids located in the outermost layer of the skin, the stratum corneum (SC) are considered to be important for the barrier. In the present study the lipid composition and lipid organization of the SC of AD dogs and control dogs were examined. The lipid composition of lesional AD skin as compared to control skin, showed a reduced free fatty acid level and a decreased ratio of ceramide[NS] C44/C34, in which C44 and C34 are the total numbers of carbon atoms of the sphingosine (S) and non-hydroxy (N) acyl chains. As a consequence of the observed changes in lipid composition in AD lesional skin the lamellar organization of lipids altered and a shift from orthorhombic to hexagonal lipid packing was monitored. Simultaneously an increased conformational disordering occurred. These changes are expected to compromise the integrity of the skin barrier. The C44/C34 chain length ratio of ceramide[NS] also showed a decreasing nonlinear relationship with the AD severity score (CADESI). Taken together, canine atopic skin showed alterations in SC lipid properties, similar to the changes observed in atopic dermatitis in humans, that correlated with a disruption of the skin barrier. Hence lipids play an important role in the pathogenesis of Canine Atopic Dermatitis.

1. Introduction

Atopic dermatitis (AD) in dogs, like in humans is a genetically predisposed chronic inflammatory and pruritic skin disease [1,2]. The pathogenesis of canine AD is not well understood and one of the paradigms is that skin barrier dysfunction may facilitate allergen penetration into the epidermal layers and subsequently induction of both innate and adaptive immune responsiveness causing clinical symptoms in sensitive individuals [1,3]. This may further deteriorate the barrier function, influence the microbiome of the skin and may lead to exacerbation of clinical symptoms as observed in AD in humans [4–6].

The stratum corneum (SC), the outermost layer of the epidermis, acts as the primary physical barrier of the skin. The “brick and mortar” structure of the SC consists of corneocytes (the bricks) embedded in a lipid matrix (the mortar) [7]. Integrity of the SC, particularly the lipid matrix, is important in maintaining the skin barrier function [8–11]. Previous studies have shown changes in lipid properties in non-lesional and lesional skin of human AD [9,12–16]. The main lipid classes are ceramides (CERs), free fatty acids (FFAs) and cholesterol (CHOL) [17–19]. Studies of human SC revealed that CERs, FFAs and CHOL assemble in two crystalline lamellar phases with repeat distances of approximately 6 and 13 nm, referred to as the short (SPP) and long periodicity phases (LPP), respectively [20,21]. The lipids within the lamellae may be organized in an orthorhombic lateral packing (very dense), a hexagonal lateral packing (less dense) or a liquid packing (high conformational disordering). Whereas the orthorhombic pattern is most abundantly present in SC of healthy human skin, it was shown that the fraction of lipids forming a hexagonal lateral packing is increased in SC of AD skin compared to that in control skin [9,14,22]. The altered lipid organization in AD skin can be correlated with the changes in lipid composition in the SC [23]. In more detail, a reduction in the skin barrier function in AD patients correlated with i) a decrease in total lipid content in SC [13,24], ii) a reduced chain length of the FFAs and the CERs [9,14], iii) an increase in the fraction of lipids forming a

Abbreviations: AD, atopic dermatitis; CADESI, Canine Atopic Dermatitis Extent and Severity Index; CT, control skin; NLS, non-lesional atopic skin; LS, lesional atopic skin

* Corresponding author at: Department of Companion Animals Clinical Sciences, Faculty of Veterinary Medicine, Kasetsart University, Bangkok, Thailand.
E-mail addresses: s.chermprapai@uu.nl, fvetstw@ku.ac.th (S. Chermprapai), f.broere@uu.nl (F. Broere), gooris_g@lacdr.leidenuniv.nl (G. Gooris), y.m.schlotter@uu.nl (Y.M. Schlotter), v.rutten@uu.nl (V.P.M.G. Rutten), bouwstra@lacdr.leidenuniv.nl (J.A. Bouwstra).

https://doi.org/10.1016/j.bbamem.2017.11.013
Received 3 August 2017; Received in revised form 17 November 2017; Accepted 20 November 2017
Available online 22 November 2017

hexagonal packing [9].

Currently only limited information is available concerning the lipid composition [6,25] and lipid organization [26–28] in SC of dog skin. Since in humans the impaired skin barrier plays an important role in the pathogenesis of AD, in the present study we examined the lipid composition, the lamellar and lateral organization in SC of lesional and non-lesional skin of AD dogs as well as control animals. Lesional atopic skin showed changes in the lipid composition and organization similar to those observed in atopic dermatitis in humans.

2. Material and methods

2.1. Animals

Three control dogs and five AD dogs were included in this study. The control Beagle dogs, owned by the Utrecht University Animal facility unit, aged between 1 and 3 years. The AD dogs (Bedlington beagle crossbreeds), owned by the Department of Clinical Sciences of Companion Animals, Faculty of Veterinary Medicine, Utrecht University, aged between 2 and 9 years. The atopic dogs met the diagnostic criteria for AD and other causes of pruritus were ruled out [29]. The severity of AD lesions was evaluated by the third version of the CADESI (Canine Atopic Dermatitis Extent and Severity Index) at each site (local score) and 62 body sites (total score) as described previously [30,31].

2.2. Skin biopsies and SC isolation

Prior to taking biopsies of the skin, hair was shaved at two sites that are commonly lesional in AD dogs (axilla and inguinal) and one site commonly non-lesional (trunk). Skin biopsies (10×10 cm^2) of both control and AD dogs were taken, by surgical blade excision immediately after euthanasia for purposes unrelated to this study. The SC was isolated from skin biopsies with small modifications of the method described by Tanojo et al. [32]. Briefly, subcutaneous fat was removed and the remaining part of the skin was stretched on a polystyrene foam block. A dermatome was used to cut the skin at the proper thickness of 0.3–0.6 mm. The dermatomized skin was collected on filter paper soaked with 0.1% trypsin solution (in PBS) in a petri dish at 4 °C. After 24 h, dishes were placed at 37 °C for 3 h and the SC was peeled off from the epidermis at room temperature. Subsequently the SC was washed with 0.1% trypsin inhibitor solution (in PBS) and stored at room temperature in a plastic bag containing silica gel and argon gas until further analyses.

2.3. Small angle X-ray diffraction

To examine the lamellar lipid organization in SC, small angle X-ray diffraction (SAXD) was used. Measurements were performed at the European Synchrotron Radiation Facility (ESRF, Grenoble, France) at station BM26B. Prior to the measurements, the SC was hydrated for 24 h over a solution of 27% NaBr. The SAXD patterns were detected with a Pilatus 1 M detector (1043×981 pixels) and a sample to detector distance of 2 m, for a period of 2×150 s. The scattering profile of the X-rays of the SC samples was recorded as a function of its scattering vector (q) defined by $q = 2\pi \sin\theta/\lambda$ (λ is the wavelength of the X-rays, either 0.1033 or 0.124 nm, and θ is the angle of the scattered X-rays) [33]. The diffraction pattern of a lamellar phase is characterized by a series of equidistant peaks. The position of each peak can be denoted by its q-value or by its corresponding spacing, which is equal to $2\pi/q$. When dealing with a lamellar phase, the diffraction peaks attributed to such a phase are located at an equidistant position in the diffraction curve. This means that the nth order peak is located at a q-value being $n.q_1$ (the position of the 1st order diffraction peak of that lamellar phase). For calibration silver behenate/Cholesterol was used.

2.4. Fourier transform infrared spectroscopy (FTIR)

To analyze the lateral lipid organization, a Varian 670-IR spectrometer equipped with a broad band mercury-cadmium-telluride detector was used and the spectral resolution was 1 cm^{-1}. Absorption of infrared light of wavelengths ranging between 400 cm^{-1} and 4000 cm^{-1} was recorded [34]. Each spectrum was an average of 2560 scans and was collected during a temperature increase of 1 °C between 0 °C and 90 °C. Using the software Varian Resolution Pro 4.1.0.101 [35–37], all spectra were baseline-corrected and deconvoluted before analysis. After correction we focused on two regions of the spectra. To obtain information about conformational ordering of the chains, the positions of the CH_2 symmetric stretching within the wavelength range 2840–2860 cm^{-1} were determined. The changes in the position of the CH_2 symmetric stretching vibrations as function of temperature were determined as described previously [36]. The positions of the stretching vibration provide information on the conformational ordering. When the lipids are highly ordered, the CH_2 symmetric stretching frequencies are < 2850 cm^{-1}. When the lipids exhibit a high conformational disordering, the liquid phase, the peak positions of the CH_2 symmetric stretching vibrations are higher than 2853 cm^{-1}. The temperatures of the transitions from the orthorhombic to the hexagonal phase and the hexagonal to the liquid phase were determined from the plots. The midpoint temperature was taken as the transitional temperature by curve fitting with five linear functions to use a six-pair-parameter of the temperature and frequency [35].

To obtain information about the lateral packing, also the scissoring vibration in the spectrum was monitored. For CH_2 scissoring vibration, appearance of vibrations at both the frequencies 1463 and 1473 cm^{-1} (Table 1) indicate the presence of an orthorhombic phase in the sample, whereas the presence of vibration at approximately 1467 cm^{-1} only, represents a hexagonal or liquid phase.

2.5. Lipid extraction

To determine the lipid composition, SC lipids were extracted by the method described by Thakoersing et al. [40] using a modified Bligh and Dyer extraction procedure. The organic phases collected were dried under a stream of nitrogen gas at 40 °C dissolved in chloroform: methanol (2:1) and stored at − 20 °C.

2.6. High performance thin layer chromatography (HPTLC) and mass spectrometry (MS)

The lipid composition focusing on CERs, FFAs and CHOL present in the SC were analyzed by HPTLC. Using this approach 8 different CER subclasses or combinations of subclasses can be separated. CERs consist of a sphingoid base and an acyl chain, nomenclature according to Motta et al. [41]. The base can be either sphingosine (denoted by S), phytosphingosine (P), 6-hydroxyspingosine (H) or dihydroxysphingosine (dS), the acyl chain is either non-hydroxy (N), α-hydroxy (A) or ω-hydroxy acyl chain ester linked to a linoleate (EO). Hence CER subclasses to be distinguished are CER[EOS], CER[NS/NdS], CER[EOP], CER[NP], CER[EOH], CER[AS/NH], CER[AP], CER[AH] [42,43], in which CER[NS] and CER[NdS] together with CER[AS] and CER[NH]

Table 1
The most prominent infrared absorption frequency regions in FTIR analyses [10,38,39].

Frequency/cm^{-1}	Assignment	Remarks
2846–2855	CH_2 symmetric stretching	Frequency increases when chain becomes disordered
1463 and 1473	CH_2 scissoring	Orthorhombic phase
1467	CH_2 scissoring	Hexagonal phase
1466	CH_2 scissoring	Disordered phase

cannot be separated with HPTLC. The extracted lipids were assessed according to the method of Thakoersing et al. [40] and Ponec et al. [44]. Briefly, samples that were dissolved in chloroform: methanol (2:1) were reconstituted individually at a concentration of 1 mg/ml of lipids and 40, 80 and 120 μg quantities were sprayed on the HPTLC plate (silica gel 60, Merck, NJ, USA) using a CAMAG Linomat IV device (Muttenz, Switzerland). A synthetic lipid mixture at a concentration of 1 mg/ml was used as a standard for the lipid identification and quantification. These calibration samples (standard) were applied in different quantities (2, 4, 6, 8, 10, 15 and 20 μg) next to the experimental samples. The standard mixture consisted of 0.318 μg/ml of CHOL, 0.318 of μg/ml FFAs (C16, C18, C20, C22, C23, C24 and C26), 0.064 μg/ml of CER[EOS], 0.042 μg/ml of CER[EOP], 0.093 μg/ml each of CER[NS], CER[NP] and CER[AS], 0.038 μg/ml of CER[AP]; and 0.053 μg/ml of cholesterol sulphate. Separation of lipid classes and subclasses was established using four different solvent mixtures according to the procedure of Ponec et al. [44]. Subsequently the plate was dried and stained with $CuSO_4$/Cu $(AcO)_2$ mixture and charred at 80 °C (CHOL and its sterol derivatives are visible) and 170 °C (all the saturated compounds are visible). Finally, the HPTLC plate was scanned and data analyzed. The calibration curves for all the compounds of the synthetic standard mixture were calculated using GraphPad Prism 6.05. Using the calibration curves of the individual lipid classes and CER subclasses, the quantities of CHOL, FFAs and CER subclasses in the experimental samples were calculated.

Samples were also analyzed by chromatography combined with mass spectrometry (LC/MS) using an Acquity UPLC H-class (Waters, Milford, MA, USA) connected to an XEVO TQ-S mass spectrometer (Waters, Milford, MA, USA). Samples were run using full scan analysis in positive ion mode (350–1200 *m/z*) under atmospheric pressure chemical ionization (APCI) as described elsewhere [45]. Separation was performed on a pva-silica column (5 μm particles, 100 × 2.1 mm i.d.; YMC, Kyoto, Japan). As an internal standard CER[NS] with a protiated sphingoid base and a deuterated acyl chain with 24 carbon atoms was used. From the ion maps the peak areas corresponding to CER[NS] and CER[NdS] with a total hydrocarbon chain length of 34 carbon atoms were integrated and compared to the CER[NS] and CER[NdS] with a total chain length of 44 carbon atoms respectively.

2.7. Statistical analyses

Mean, standard deviation (SD) and standard error of the mean (SEM) were calculated with GraphPad Prism 6.05. Non-parametric tests: independent samples Kruskal-Wallis corrected by Dunn's multiple comparisons testing were used for comparison between any contrasts of non-lesional AD, lesional AD and control sample groups, and analyzed by GraphPad Prism 6.05 and Stata. The correlation between the carbon chain length of CER[NS] and AD severity score (CADESI) was tested by Spearman rank-order correlation.

3. Results

3.1. Overview of dog skin samples

All control and non-lesional AD skin samples were taken from the trunk area and the local CADESI scores were zero for each of these (Table 2). Lesional AD skin samples were mostly taken from the axilla and inguinal region, well-defined predilection sites according to the study of Favrot et al. [46] clearly presenting the highest local AD severity scores in our study as well (Table 2). One of the AD dogs also presented clear lesions at the trunk, these data were included in analyses of the lesional tissue group of this study.

3.2. Lamellar organization in SC of dog skin analyzed by SAXD

To determine whether changes occurred in the lamellar organization, diffraction patterns of SC of AD dogs and those of control animals were measured. Focusing on the diffraction patterns of control SC, a strong peak (II) is located at a q-value of 1.0 nm^{-1} corresponding to a spacing of 6.4 nm (Fig. 1A). This peak is attributable to the 1st order diffraction of the SPP and the 2nd order diffraction peak of the LPP, as explained for human SC previously [9]. On the right-hand-side of this strong peak, a shoulder (III) is located at a q value of approximately 1.3 nm^{-1} corresponding to a spacing of 4.7 nm, attributed to the LPP being the 3rd order diffraction peak of this phase. A shoulder (I) is located at 0.5 nm^{-1} (not shown in Fig. 1A) and it is attributed to the LPP as the 1st order diffraction peak. A sharp peak (*) at a q-value of approximately 1.88 nm^{-1} (spacing of 3.34 nm) is due to the phase separated crystalline CHOL. On the right-hand side of this sharp peak a weak shoulder is located, which can be attributed to the 2nd order diffraction peak of the SPP and/or the 4th order diffraction peak of the LPP. When comparing the curves of the three control samples, the peak positions do not vary. However, a variation is observed in intensity of the shoulder (peak III) and of the peak attributed to phase separated CHOL (*).

When focusing on the diffraction patterns of SC lipids from non-lesional AD samples (Fig. 1B) slight variations were observed compared to the controls: i) the spacing corresponding to the position of the strongest peak (II) varies between 6.3 and 6.5 nm, ii) a weaker intensity of the shoulder indicated by III, iii) an additional peak (denoted by A) was shown in two out of four diffraction patterns (NLS1 and NLS4) at a q-value of approximately 0.75 nm^{-1} corresponding to a spacing of around 8.5 nm.

The diffraction patterns of lesional AD skin (Fig. 1C) showed features also observed in the diffraction patterns of SC from non-lesional skin, though with weaker diffraction peaks. Differences in the diffraction patterns as compared to control skin are more pronounced. The most important being i) variation in the position of the strong diffraction peak (II), spacing varying between 6.2 and 6.5 nm, ii) a weaker intensity of both, the phase separated CHOL peak (denoted by *) and the shoulder denoted by III was observed, iii) an additional diffraction peak (denoted by A) corresponding to a spacing of around 8.5 nm was observed in the patterns of LS2 and LS3, iv) a 2nd additional peak (denoted by B) was observed at a spacing of approximately 5.4 nm in the diffraction curve of LS7.

3.3. Lateral organization in SC of dog skin analyzed by FTIR

To examine the lateral packing of the lipids, FTIR spectra from isolated SC of AD dogs were monitored and compared to controls. To determine the conformational ordering, CH_2 symmetric stretching frequencies in the infrared spectra of SC were recorded between 0 °C and 90 °C with a continuous temperature increment. In SC of control skin, at 0 °C, the CH_2 symmetric stretching frequencies were 2848.6 cm^{-1} which gradually increased when increasing the temperature (Fig. 2A). The thermotropic response curve of the CH_2 symmetric stretching vibrations of control SC showed prominent shifts at approximately 35–45 °C and 70–80 °C indicating two-phase transitions, the orthorhombic-hexagonal and hexagonal-liquid phase transitions, respectively (Fig. 2A).

The CH_2 symmetric stretching frequency in the spectrum of SC of non-lesional AD skin was 2848.9 cm^{-1} at 0 °C, slightly higher than the frequency of control skin at the same temperature (Fig. 2A). The frequency gradually shifted to higher values at increasing temperatures and remained higher than those of control skin in the whole temperature range. The curve of non-lesional AD also showed two prominent shifts in the CH_2 symmetric stretching frequencies at approximately 35–45 °C and 60–75 °C representing the two phase transitions but the shifts were less prominent than those observed in the thermotropic response curve of the control skin (Fig. 2A).

The thermotropic response curve of SC of lesional AD skin started at 2849.1 cm^{-1} and when increasing the temperature frequencies were

Table 2
Skin sample characteristics. An overview of skin samples (CT: control; NLS: non-lesional AD; LS: lesional AD) used in the present study and their characteristics.

Skin group	Dog	Sampling Site	Local CADESI-score		Total CADESI-score		Duration of clinical signs
			Local score[b]	Severity	Total score[a]	Severity	
Control1 (CT1)	D1	Trunk	0	None	0	None	–
Control2 (CT2)	D2	Trunk	0	None	0	None	–
Control3 (CT3)	D3	Trunk	0	None	0	None	–
Non-lesional1 (NLS1)	D4	Trunk	0	None	< 16	Remission	–
Non-lesional2 (NLS2)	D5	Trunk	0	None	< 16	Remission	–
Non-lesional3 (NLS3)	D6	Trunk	0	None	37	Mild	–
Non-lesional4 (NLS4)	D7	Trunk	0	None	61	Moderate	–
Lesional1 (LS1)	D6	Axilla	1	Mild	37	Mild	2 mo.
Lesional2 (LS2)	D7	Axilla	2	Moderate	61	Moderate	2 mo.
Lesional3 (LS3)	D8	Axilla	3	Moderate	116	Moderate	3 mo.
Lesional4 (LS4)	D6	Inguinal	2	Moderate	37	Mild	2 mo.
Lesional5 (LS5)	D7	Inguinal	2	Moderate	61	Moderate	2 mo.
Lesional6 (LS6)	D8	Inguinal	3	Moderate	116	Moderate	3 mo.
Lesional7 (LS7)	D8	Trunk	3	Moderate	116	Moderate	3 mo.

[a] Total score (1240 maximum):0–15: remission; 16–59: mild AD; 60–119: moderate AD; ≥ 120: severe AD.
[b] Local score: 0: none; 1: mild; 2–3: moderate; 4–5: severe.

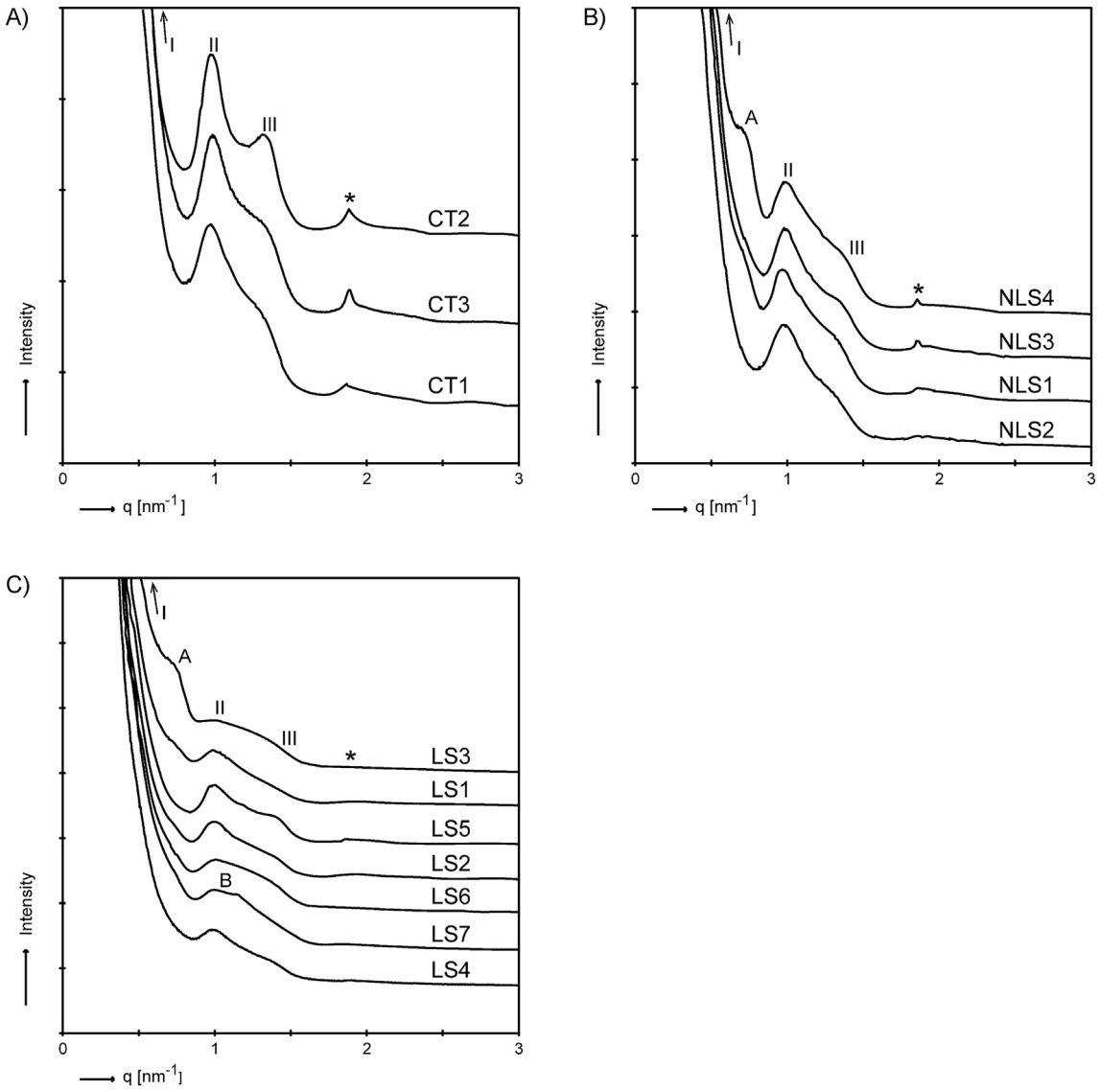

Fig. 1. The diffraction patterns of SC from skin of control dogs, and non-lesional and lesional skin of AD dogs. Small angle X-ray diffraction (SAXD) patterns of SC isolated from A) control (CT) skin (n = 3); B) non-lesional (NLS) skin of AD dogs (n = 4); and C) lesional (LS) skin of AD dogs (n = 7), as described in detail in Table 2. Represented are I: the first order diffraction peak of LPP, II: the combination of the first order diffraction peak of the SPP and the second order diffraction peak of the LPP, III: the third order diffraction peak of LPP. The star (*) represents the diffraction peak of phase separated crystalline CHOL. See more detail of the typical SAXD profile in Janssens et al. [9].

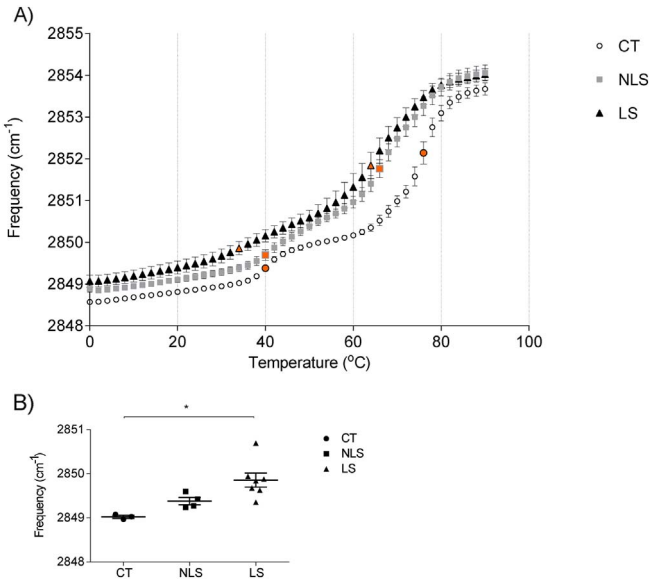

Fig. 2. Conformational ordering of the hydrocarbon chains in the SC of dog skin as analyzed by FTIR. Thermotropic response of the CH_2 symmetric stretching frequencies in a temperature range between 0 and 90 °C. A) Thermotropic response of the CH_2 stretching frequencies ± SEM cm^{-1} in SC isolated from control (CT, n = 3), non-lesional AD (NLS, n = 4) and lesional AD (LS, n = 7) dog skin. The colored symbols represented the mid-points of the transition from orthorhombic to hexagonal or hexagonal to liquid phases. B) The CH_2 symmetric stretching frequencies at a selected temperature of 34 °C. A significant difference, $p < 0.05$ (*) was observed between the average frequencies of CH_2 symmetric stretching vibrations of lesional skin (2849.9 cm^{-1}) and control skin (2849.0 cm^{-1}). (For interpretation of the references to color in this figure legend, the reader is referred to the web version of this article.)

higher as compared to those of non-lesional AD skin and control skin in the temperature range of 0–80 °C (Fig. 2). The first shift in the CH_2 symmetric stretching frequencies at approximately 35–45 °C was not very prominent (Fig. 2A). The second shift in CH_2 symmetric stretching frequencies was detected at approximately 60–70 °C with the average mid-point temperatures and frequencies shown in Fig. 2A. The average mid-point temperatures and frequencies of the transition from the orthorhombic to hexagonal phase and of the transition from hexagonal to liquid phase in control samples (n = 3), non-lesional samples (n = 4) and lesional samples (n = 7) are provided in Table 3. The CH_2 symmetric stretching frequency of control, non-lesional and lesional AD skin at 34 °C shown in Fig. 2B, was chosen since dog skin temperature is reported to be approximately 34.5–35.5 °C [47,48].

To obtain more detailed information about the orthorhombic and hexagonal lateral packing of lipids in SC, also the CH_2 scissoring frequencies in the FTIR spectra were analyzed between 0 and 60 °C. In control skin, two peaks in the scissoring vibrations were clearly visible below 40 °C at 1463 and 1473 cm^{-1} (Fig. 3A), demonstrating that a large fraction of lipids was assembled in an orthorhombic packing. However, as a weak peak at 1467 cm^{-1} is also present, it cannot be excluded that a small fraction of lipids adopted a hexagonal packing at temperatures below 34 °C. Between 34 °C and 44 °C the intensity of the scissoring frequency at 1467 cm^{-1} increased at the expense of the intensities of the frequencies at 1463 and 1473 cm^{-1}, representing the transition from the orthorhombic to the hexagonal phase. When focusing on the scissoring frequencies in the spectrum obtained from SC of non-lesional AD skin at low temperatures, the two peaks at 1463 and 1473 cm^{-1} are clearly present, indicating the presence of an orthorhombic phase (Fig. 3B), similarly as in the spectrum of the control SC. In this example the orthorhombic to hexagonal phase transition occurred between 38 °C and 46 °C. The scissoring frequencies in the spectrum of lesional skin are clearly different. At low temperature, the two scissoring frequencies indicating the orthorhombic lateral packing are still present at 1463 cm^{-1} and 1473 cm^{-1}, but the intensity is much weaker than in control and non-lesional SC (Fig. 3C). This demonstrates that a substantial smaller fraction of lipids is assembled in an orthorhombic packing. Furthermore, at low temperatures, the scissoring vibration at 1467 cm^{-1} is prominently present, suggesting that a large fraction of lipids adopted a hexagonal packing. When increasing the temperature, the transition from an orthorhombic to hexagonal packing takes place at much lower average temperatures as compared to the control and non-lesional AD skin, the orthorhombic phase disappeared already at approximately 34 °C (Fig. 3D–F).

3.4. Lipid composition in SC of dog skin analyzed by HPTLC and mass spectrometry

Focusing on the individual lipid classes in SC, no significant differences were observed between AD (both non-lesional and lesional) and control samples in the relative abundance of CHOL, total CERs (Fig. 4A) and CER subclass (Fig. 4B). In contrast, the relative abundance of FFAs was significantly lower in lesional AD (9.6 ± 1.4%) compared to control samples (13.9 ± 1.0%) ($p < 0.05$) (Fig. 4A). The percentage of CER[EOS], CER[NS/NdS] and CER[AS/NH] subclasses were the most predominant of the total CERs content in control dog SC as well as in AD skin (Fig. 4B).

Using LC/MS the C44/C34 chain length of two CER subclasses, CER [NS] and CER[NdS] were examined as CER[NS] and CER[NdS] with a chain length of C34 were increased in AD human skin compared to controls [9,14]. The present analyses showed a significant reduction in the ratio of the peak areas of CER[NS] C44/C34 species in lesional SC of AD skin compared to control SC, while the peak area ratio of C44/C34 of CER[NdS] was not different between the groups (Fig. 5A). In addition, we studied the association between the peak area ratio of C44/C34 of CER[NS] with the CADESI score (Fig. 5B). A decreasing nonlinear relationship between the CER[NS] C44/C34 and the CADESI score was observed (Spearman rank test correlation at $p = 0.041$, two-sided) (Fig. 5B). The AD skin with the moderate CADESI score (non-lesional AD) showed a lower ratio (5–25) of C44/C34 CER[NS] compared to control skin and the ratio was even less (0 − 12) for AD skin with the high CADESI score (lesional AD).

Table 3
CH_2 stretching frequencies and midpoint transition temperatures. The midpoint transition temperatures are based on the thermotropic response curves obtained from spectra of SC. Data shown in mean ± SEM. Significant differences between groups ($p < 0.05$, $p < 0.01$, $p < 0.005$ denoted by *, **, ***, respectively) were tested by non-parametric Kruskal Wallis and Dunn's multiple comparison, N.S.: no statistical significance.

Group		Control (CT, n = 3)	Non-lesional (NLS, n = 4)	Lesional (LS, n = 7)	Comparison
CH_2 stretching orthorhombic-hexagonal phase	Frequency (cm^{-1})	2849.4 ± 0.0	2849.8 ± 0.1	2849.8 ± 0.1	NLS vs CT* LS vs CT*
	Transitional temperature (°C)	40.3 ± 0.3	41 ± 0.8	35 ± 1.5	NLS vs LS** LS vs CT*
CH_2 stretching hexagonal-liquid phase	Frequency (cm^{-1})	2852.3 ± 0.1	2851.9 ± 0.2	2852 ± 0.2	N.S.
	Transitional temperature (°C)	76.3 ± 0.7	66.5 ± 0.5	64.6 ± 1.4	NLS vs CT* LS vs. CT***

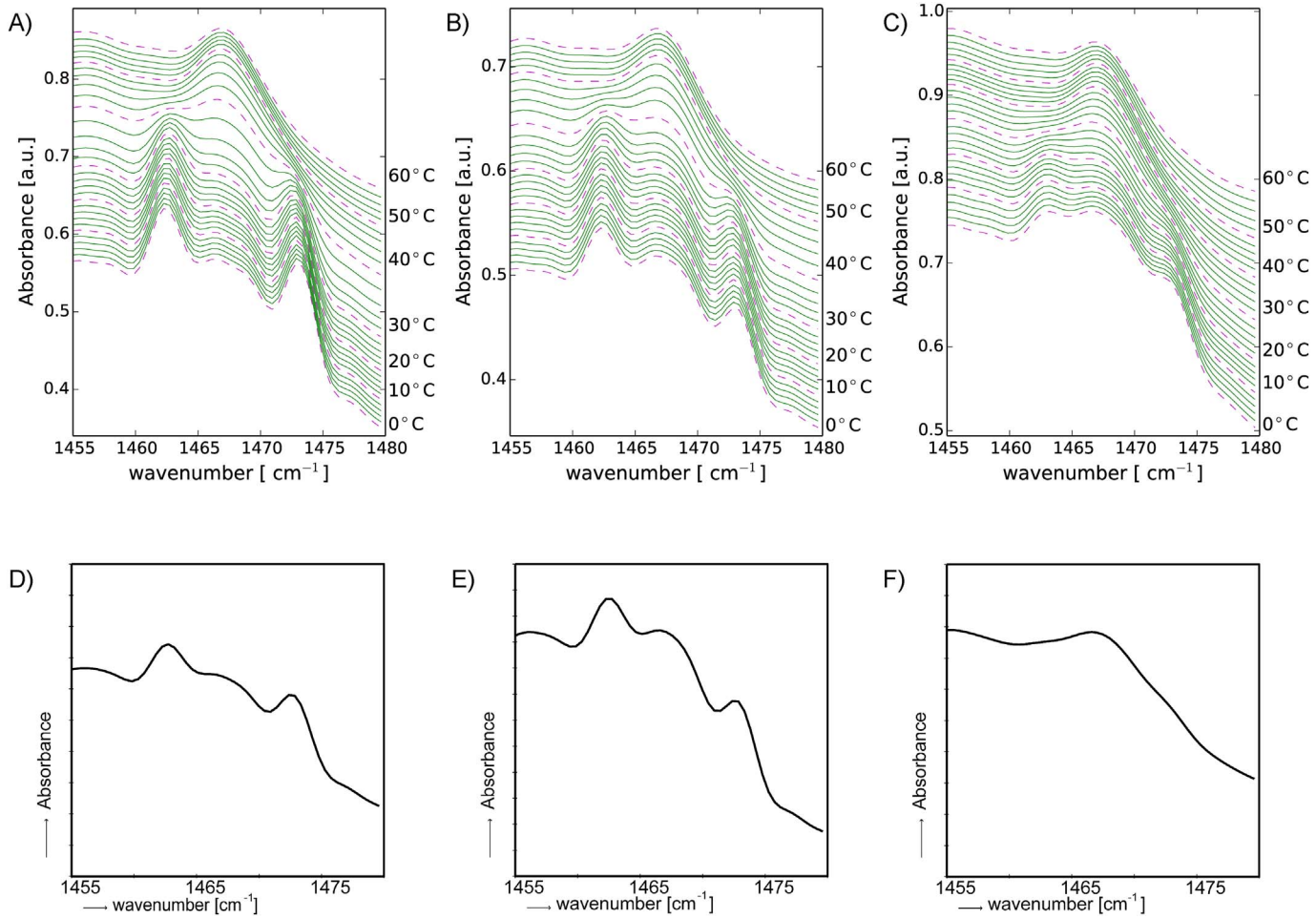

Fig. 3. Representative examples of the scissoring vibrations (1460–1480 cm^{-1}) in the infrared spectra of SC. Data shown are frequency spectra at temperatures between 0 °C and 60 °C (top row) and at 34 °C (bottom row) of control (A and D, respectively); non-lesional AD (B and E, respectively) and lesional AD (C and F, respectively) skin samples.

4. Discussion

Since the exact pathogenesis of AD remains unclear and the primary cause is controversial, various hypotheses are under debate [4,5]. The present study is based on the paradigm that skin barrier abnormalities might be the etiological factors that facilitate triggering AD. Since lipids, besides proteins are crucial components of the skin barrier [8–10], alterations in lipid composition in the SC may change the lipid organization and thus the skin barrier function. Therefore, the focus of this study was to examine whether the lipid properties of the SC of non-lesional and lesional AD dog skin were different from those of SC of control dog skin.

In literature, only limited data is available about the lipid organization in the SC of AD dogs. In previous studies ultra-structural assessment of SC of canine AD skin suggested higher disordering in the lipid lamellae in both non-lesional and lesional samples, in the limited number of electron microscopic images analyzed [26–28]. In our study we used X-ray diffraction to examine the lamellar organization. This bulk technique measures general changes but is unable to monitor local disordering of the lamellar phases in SC of AD dog skin. In addition, lipid analysis using HPTLC and LC/MS revealed a reduced amount of total free CER in SC in lesional skin compared with control skin [6,49,50]. With respect to the two other major lipid classes FFAs and CHOL in SC, whereas one study reported no differences in the relative levels between lesional and control skin [50], another one reported lower amounts of FFAs and CHOL presented as weight per weight SC in AD skin [49]. Some of the observed discrepancies between literature and our current study can be due to differences within dog cohort, differences in analysis or due to the limited number of samples available for our analysis.

In the present study we examined both the lipid composition and the lipid organization in SC. We did not observe changes in the percentage of CHOL and CERs, including CER subclasses, but a reduced level of FFAs was observed in lesional AD compared to control skin. Furthermore, the ratio of C44/C34 of CER[NS] was drastically decreased in AD lesional skin. These changes in lipid composition have had consequences for the lipid organization as discussed below.

The lamellar organization in SC of non-lesional skin differed slightly from that in control animals, whereas lesional AD skin revealed a more prominent variation in the main peak position as well as a weaker shoulder in the SAXD patterns attributed to LPP, indicating changes in the lamellar phases and possibly decreased formation of LPP. The reduction in LPP formation results in an increased permeability of the skin barrier [8] and therefore the observed changes in the present study may contribute to a reduced skin barrier function. In previous studies it was observed that an increase in the level of CERs with a total chain length of C34 resulted in a reduction in the spacing [36,51]. Hence the observed drastic reduction in the ratio C44/C34 in CER[NS], the most abundant CER subclass in dog skin, may contribute to a change in the lamellar phases. The changes observed in the lamellar organization in SC of lesional skin of AD dogs are consistent with earlier studies in human AD skin [9,12]. Nonetheless, in those studies no additional peak corresponding to a spacing of 8.5 nm was observed. This peak may be due to dog hair that could not fully be removed since X-ray diffraction of only hairs revealed a diffraction peak at approximately 8.5 nm spacing.

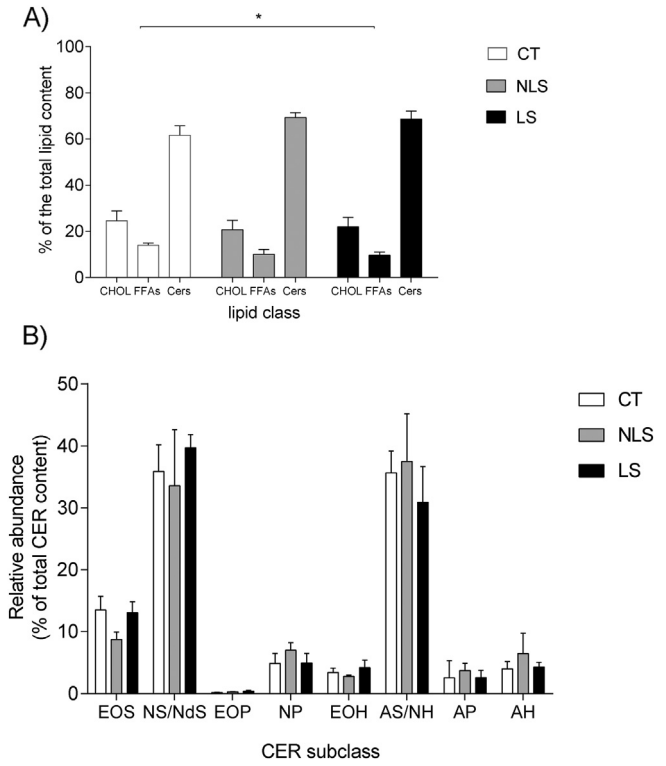

Fig. 4. The lipid composition of dog SC. The lipid composition of dog SC was analyzed by HPTLC. Represented are A) the percentages of major lipid classes: CHOL, FFAs and CERs (= sum of CER subclasses) and B) the abundance in percentage of each CER (sub) class: [EOS], [NS/NdS], [EOP], [NP], [EOH], [AS/NH], [AP], [AH] as compared to the total CER content. Data shown in mean ± SD of control (CT, n = 3), non-lesional AD (NLS, n = 3) and lesional AD (LS, n = 7) skin samples. Significant differences compared to the control ($p < 0.05$, denoted by *) were tested by non-parametric Kruskal Wallis and Dunn's multiple comparison.

The lateral packing of lipids in SC was examined by FTIR. Higher conformational disordering was indicated by an increase in the frequencies of CH_2 symmetric stretching vibrations in a large temperature range in lesional AD and non-lesional AD compared to control skin. In addition, measuring the CH_2 scissoring vibrations indicated that in SC of AD lesional skin the fraction of lipids assembled in an orthorhombic packing was reduced compared to that in SC of control dog skin. This was confirmed by analyses of rocking vibrations (not shown, frequencies 728 and 720 cm^{-1}). Studies performed in lipid model systems, showed that a reduction in FFAs level and a reduction in chain length of CERs resulted in the fraction of lipids assembled in a hexagonal lateral packing rather than orthorhombic packing [37,52]. Therefore, the observed reduction in FFAs level and/or ratio CER[NS] C44/C34 may have contributed to hexagonal lipid organization in lesional skin in AD dog.

The increase in conformational disordering and the more prominent presence of lipids assembled in a hexagonal packing observed in SC of lesional skin of AD dogs are in agreement with findings in human AD skin as described previously [9,14,22]. Moreover, a correlation between the level of C34 and the severity of AD (SCORAD) in humans [9] was also indicated in the present study in canine AD (CADESI score). The latter indicates that the reduced chain length of CER are relevant not only in the lipid organization, hence barrier integrity, but as a consequence may also be correlated with the severity of the disease.

5. Conclusion

In the present study we examined the lipid composition, the lamellar organization and the lateral organization of the lipids in SC in lesional and non-lesional skin of AD dogs as well as in control dogs. Our data show that the alterations in lipid properties of SC in atopic skin of dogs are similar to changes in the lipid composition and organization observed in atopic dermatitis in humans [9,12,14,22], impair the physical integrity of SC, resulting in an impaired skin barrier. The loss of barrier function allows allergens and pathogens to easily penetrate the skin, which triggers the disease. Interestingly in humans as well as in dogs a correlation has been observed between the severity of the disease and the level of CERs with a total chain length of C34. A better understanding of the pathogenesis of canine AD will be beneficial to the improvement of therapeutic strategies of this skin disorder.

Transparency document

The Transparency document associated with this article can be found, in the online version.

Acknowledgements

We would like to thank Hans J.C.M. Vernooij for his statistical analyses support, the scientist of the Dubble beamline BM26B at the ESRF (Grenoble, France) for their assistance and the allocation of beam time for the X-ray diffraction measurements and Rianne van Dijk for

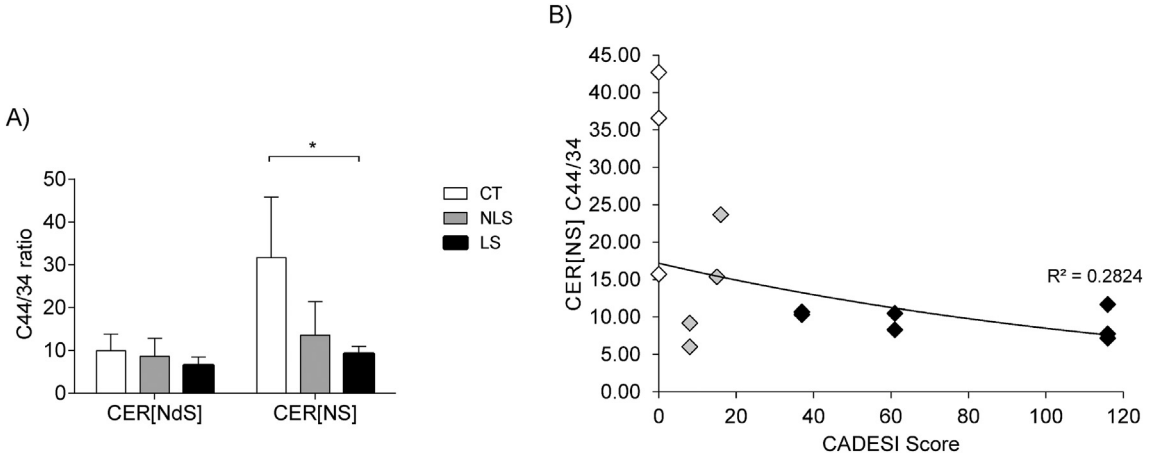

Fig. 5. The correlation between CER chain length and AD dog SC. A) The data shown in mean ± SD of C44/C34 ratio of CER subclasses in control (CT, n = 3), non-lesional AD (NLS, n = 4) and lesional AD (LS, n = 7) dog skin samples. Significant differences compared to the control ($P < 0.05$, denoted by *) were tested by non-parametric Kruskal Wallis and Dunn's multiple comparison. B) The correlation between the C44/C34 ratio of CER[NS] and the CADESI score of dog skin types: control indicated by ◇, non-lesional AD indicated by ◈, lesional AD indicated by ◆; raw data were log-transformed and tested by Spearman rank-order correlation at $p < 0.05$.

performing the LC/MS measurements. This study was financially supported by a scholarship from Faculty of Veterinary Medicine, Kasetsart University, Bangkok, Thailand.

Conflict of interest

The authors have no conflicts of interest.

References

[1] T. Olivry, D.J. DeBoer, C.E. Griffin, R.E. Halliwell, P.B. Hill, A. Hillier, R. Marsella, C.A. Sousa, The ACVD task force on Canine Atopic Dermatitis: forewords and lexicon, Vet. Immunol. Immunopathol. 81 (2001) 143–146.

[2] Y.M. Schlotter, V.P. Rutten, F.M. Riemers, E.F. Knol, T. Willemse, Lesional skin in atopic dogs shows a mixed Type-1 and Type-2 immune responsiveness, Vet. Immunol. Immunopathol. 143 (2011) 20–26.

[3] C.E. Griffin, D.J. DeBoer, The ACVD task force on Canine Atopic Dermatitis (XIV): clinical manifestations of Canine Atopic Dermatitis, Vet. Immunol. Immunopathol. 81 (2001) 255–269.

[4] N. Novak, D.Y.M. Leung, Role of barrier dysfunction and immune response in atopic dermatitis, in: D.Y.M. Leung, H. Sampson (Eds.), Pediatric Allergy: Principles and Practice, W.B. Saunders, Edinburgh, 2010, pp. 552–563.

[5] P.M. Elias, M. Steinhoff, "Outside-to-inside" (and now back to "outside") pathogenic mechanisms in atopic dermatitis, J. Invest. Dermatol. 128 (2008) 1067–1070.

[6] J.S. Yoon, K. Nishifuji, A. Sasaki, K. Ide, J. Ishikawa, T. Yoshihara, T. Iwasaki, Alteration of stratum corneum ceramide profiles in spontaneous canine model of atopic dermatitis, Exp. Dermatol. 20 (2011) 732–736.

[7] S.K. Chandrasekaran, J.E. Shaw, Factors influencing the percutaneous absorption of drugs, Curr. Probl. Dermatol. 7 (1978) 142–155.

[8] M. de Jager, W. Groenink, R. Bielsa, i Guivernau, E. Andersson, N. Angelova, M. Ponec, J. Bouwstra, A novel in vitro percutaneous penetration model: evaluation of barrier properties with p-aminobenzoic acid and two of its derivatives, Pharm. Res. 23 (2006) 951–960.

[9] M. Janssens, J. van Smeden, G.S. Gooris, W. Bras, G. Portale, P.J. Caspers, R.J. Vreeken, T. Hankemeier, S. Kezic, R. Wolterbeek, A.P. Lavrijsen, J.A. Bouwstra, Increase in short-chain ceramides correlates with an altered lipid organization and decreased barrier function in atopic eczema patients, J. Lipid Res. 53 (2012) 2755–2766.

[10] F. Damien, M. Boncheva, The extent of orthorhombic lipid phases in the stratum corneum determines the barrier efficiency of human skin in vivo, J. Invest. Dermatol. 130 (2010) 611–614.

[11] D. Groen, D.S. Poole, G.S. Gooris, J.A. Bouwstra, Is an orthorhombic lateral packing and a proper lamellar organization important for the skin barrier function? Biochim. Biophys. Acta 1808 (2011) 1529–1537.

[12] M. Janssens, J. van Smeden, G.S. Gooris, W. Bras, G. Portale, P.J. Caspers, R.J. Vreeken, S. Kezic, A.P. Lavrijsen, J.A. Bouwstra, Lamellar lipid organization and ceramide composition in the stratum corneum of patients with atopic eczema, J. Invest. Dermatol. 131 (2011) 2136–2138.

[13] G. Imokawa, A. Abe, K. Jin, Y. Higaki, M. Kawashima, A. Hidano, Decreased level of ceramides in stratum corneum of atopic dermatitis: an etiologic factor in atopic dry skin? J. Invest. Dermatol. 96 (1991) 523–526.

[14] J. van Smeden, M. Janssens, E.C. Kaye, P.J. Caspers, A.P. Lavrijsen, R.J. Vreeken, J.A. Bouwstra, The importance of free fatty acid chain length for the skin barrier function in atopic eczema patients, Exp. Dermatol. 23 (2014) 45–52.

[15] J.M. Jungersted, J.K. Hogh, L.I. Hellgren, G.B. Jemec, T. Agner, Ethnicity and stratum corneum ceramides, Br. J. Dermatol. 163 (2010) 1169–1173.

[16] J. Ishikawa, H. Narita, N. Kondo, M. Hotta, Y. Takagi, Y. Masukawa, T. Kitahara, Y. Takema, S. Koyano, S. Yamazaki, A. Hatamochi, Changes in the ceramide profile of atopic dermatitis patients, J. Invest. Dermatol. 130 (2010) 2511–2514.

[17] J.A. Bouwstra, G.S. Gooris, K. Cheng, A. Weerheim, W. Bras, M. Ponec, Phase behavior of isolated skin lipids, J. Lipid Res. 37 (1996) 999–1011.

[18] W.M. Holleran, Y. Takagi, Y. Uchida, Epidermal sphingolipids: metabolism, function, and roles in skin disorders, FEBS Lett. 580 (2006) 5456–5466.

[19] P.W. Wertz, B. van den Bergh, The physical, chemical and functional properties of lipids in the skin and other biological barriers, Chem. Phys. Lipids 91 (1998) 85–96.

[20] J.A. Bouwstra, G.S. Gooris, J.A. van der Spek, W. Bras, Structural investigations of human stratum corneum by small-angle X-ray scattering, J. Invest. Dermatol. 97 (1991) 1005–1012.

[21] J.A. Bouwstra, G.S. Gooris, W. Bras, D.T. Downing, Lipid organization in pig stratum corneum, J. Lipid Res. 36 (1995) 685–695.

[22] G.S. Pilgram, D.C. Vissers, H. van der Meulen, S. Pavel, S.P. Lavrijsen, J.A. Bouwstra, H.K. Koerten, Aberrant lipid organization in stratum corneum of patients with atopic dermatitis and lamellar ichthyosis, J. Invest. Dermatol. 117 (2001) 710–717.

[23] J. van Smeden, J.A. Bouwstra, Stratum corneum lipids: their role for the skin barrier function in healthy subjects and atopic dermatitis patients, Curr. Probl. Dermatol. 49 (2016) 8–26.

[24] M. Janssens, J. van Smeden, G.J. Puppels, A.P. Lavrijsen, P.J. Caspers, J.A. Bouwstra, Lipid to protein ratio plays an important role in the skin barrier function in patients with atopic eczema, Br. J. Dermatol. 170 (2014) 1248–1255.

[25] L.V. Reiter, S.M. Torres, P.W. Wertz, Characterization and quantification of ceramides in the nonlesional skin of canine patients with atopic dermatitis compared with controls, Vet. Dermatol. 20 (2009) 260–266.

[26] A.O. Inman, T. Olivry, S.M. Dunston, N.A. Monteiro-Riviere, H. Gatto, Electron microscopic observations of stratum corneum intercellular lipids in normal and atopic dogs, Vet. Pathol. 38 (2001) 720–723.

[27] A. Piekutowska, D. Pin, C.A. Reme, H. Gatto, M. Haftek, Effects of a topically applied preparation of epidermal lipids on the stratum corneum barrier of atopic dogs, J. Comp. Pathol. 138 (2008) 197–203.

[28] R. Marsella, D. Samuelson, K. Doerr, Transmission electron microscopy studies in an experimental model of Canine Atopic Dermatitis, Vet. Dermatol. 21 (2010) 81–88.

[29] T. Olivry, International Task Force of Canine Atopic Dermatitis, new diagnostic criteria for Canine Atopic Dermatitis, Vet. Dermatol. 21 (2010) 123–126.

[30] T. Olivry, R. Mueller, T. Nuttall, C. Favrot, P. Prelaud, International Task Force on Canine Atopic Dermatitis, determination of CADESI-03 thresholds for increasing severity levels of Canine Atopic Dermatitis, Vet. Dermatol. 19 (2008) 115–119.

[31] T. Olivry, R. Marsella, T. Iwasaki, R. Mueller, International Task Force On Canine Atopic Dermatitis, validation of CADESI-03, a severity scale for clinical trials enrolling dogs with atopic dermatitis, Vet. Dermatol. 18 (2007) 78–86.

[32] H. Tanojo, A. Bos-van Geest, J.A. Bouwstra, H.E. Junginger, H.E. Boodé, In vitro human skin barrier perturbation by oleic acid: thermal analysis and freeze fracture electron microscopy studies, Thermochim. Acta 293 (1997) 77–85.

[33] D. Groen, G.S. Gooris, J.A. Bouwstra, New insights into the stratum corneum lipid organization by X-ray diffraction analysis, Biophys. J. 97 (2009) 2242–2249.

[34] D. de Sousa Neto, G. Gooris, J. Bouwstra, Effect of the omega-acylceramides on the lipid organization of stratum corneum model membranes evaluated by X-ray diffraction and FTIR studies (part I), Chem. Phys. Lipids 164 (2011) 184–195.

[35] M. Oguri, G.S. Gooris, K. Bito, J.A. Bouwstra, The effect of the chain length distribution of free fatty acids on the mixing properties of stratum corneum model membranes, Biochim. Biophys. Acta 1838 (2014) 1851–1861.

[36] E.H. Mojumdar, Z. Kariman, L. van Kerckhove, G.S. Gooris, J.A. Bouwstra, The role of ceramide chain length distribution on the barrier properties of the skin lipid membranes, Biochim. Biophys. Acta 1838 (2014) 2473–2483.

[37] M. Uchiyama, M. Oguri, E.H. Mojumdar, G.S. Gooris, J.A. Bouwstra, Free fatty acids chain length distribution affects the permeability of skin lipid model membranes, Biochim. Biophys. Acta 1858 (2016) 2050–2059.

[38] M. Boncheva, F. Damien, V. Normand, Molecular organization of the lipid matrix in intact stratum corneum using ATR-FTIR spectroscopy, Biochim. Biophys. Acta 1778 (2008) 1344–1355.

[39] R.N. Lewis, R.N. McElhaney, Fourier transform infrared spectroscopy in the study of lipid phase transitions in model and biological membranes: practical considerations, Methods Mol. Biol. 400 (2007) 207–226.

[40] V.S. Thakoersing, M. Ponec, J.A. Bouwstra, Generation of human skin equivalents under submerged conditions-mimicking the in utero environment, Tissue Eng. Part A 16 (2010) 1433–1441.

[41] S. Motta, M. Monti, S. Sesana, R. Caputo, S. Carelli, R. Ghidoni, Ceramide composition of the psoriatic scale, Biochim. Biophys. Acta 1182 (1993) 147–151.

[42] J. van Smeden, L. Hoppel, R. van der Heijden, T. Hankemeier, R.J. Vreeken, J.A. Bouwstra, LC/MS analysis of stratum corneum lipids: ceramide profiling and discovery, J. Lipid Res. 52 (2011) 1211–1221.

[43] Y. Masukawa, H. Narita, E. Shimizu, N. Kondo, Y. Sugai, T. Oba, R. Homma, J. Ishikawa, Y. Takagi, T. Kitahara, Y. Takema, K. Kita, Characterization of overall ceramide species in human stratum corneum, J. Lipid Res. 49 (2008) 1466–1476.

[44] M. Ponec, A. Weerheim, P. Lankhorst, P. Wertz, New acylceramide in native and reconstructed epidermis, J. Invest. Dermatol. 120 (2003) 581–588.

[45] W. Boiten, S. Absalah, R. Vreeken, J. Bouwstra, J. van Smeden, Quantitative analysis of ceramides using a novel lipidomics approach with three dimensional response modelling, Biochim. Biophys. Acta 1861 (2016) 1652–1661.

[46] C. Favrot, J. Steffan, W. Seewald, F. Picco, A prospective study on the clinical features of chronic Canine Atopic Dermatitis and its diagnosis, Vet. Dermatol. 21 (2010) 23–31.

[47] R.M. Breathnach, P.J. Quinn, K.P. Baker, T. McGeady, E. Strobl, Y. Abbott, B.R. Jones, Association between skin surface pH, temperature and *Staphylococcus pseudintermedius* in dogs with immunomodulatory-responsive lymphocytic-plasmacytic pododermatitis, Vet. Dermatol. 22 (2011) 312–318.

[48] M.V. Hoffmann, S.B. Kastner, M. Kietzmann, S. Kramer, Contact heat thermal threshold testing in beagle dogs: baseline reproducibility and the effect of acepromazine, levomethadone and fenpipramide, BMC Vet. Res. 8 (2012) (206-6148-8-206).

[49] I. Popa, N. Remoue, B. Osta, D. Pin, H. Gatto, M. Haftek, J. Portoukalian, The lipid alterations in the stratum corneum of dogs with atopic dermatitis are alleviated by topical application of a sphingolipid-containing emulsion, Clin. Exp. Dermatol. 37 (2012) 665–671.

[50] K. Shimada, J.S. Yoon, T. Yoshihara, T. Iwasaki, K. Nishifuji, Increased transepidermal water loss and decreased ceramide content in lesional and non-lesional skin of dogs with atopic dermatitis, Vet. Dermatol. 20 (2009) 541–546.

[51] V.S. Thakoersing, M.O. Danso, A. Mulder, G. Gooris, A. El Ghalbzouri, J.A. Bouwstra, Nature versus nurture: does human skin maintain its stratum corneum lipid properties in vitro? Exp. Dermatol. 21 (2012) 865–870.

[52] E.H. Mojumdar, G.S. Gooris, J.A. Bouwstra, Phase behavior of skin lipid mixtures: the effect of cholesterol on lipid organization, Soft Matter 11 (2015) 4326–4336.